Observation of light localization in modulated Bessel optical lattices

Robert Fischer[1], **Dragomir N. Neshev**[1], **Servando Lopez-Aguayo**[1,2], **Anton S. Desyatnikov**[1], **Andrey A. Sukhorukov**[1], **Wieslaw Krolikowski**[1], **and Yuri S. Kivshar**[1]

[1]*Nonlinear Physics Centre and Laser Physics Centre, Centre for Ultrahigh-bandwidth Devices for Optical Systems (CUDOS), Research School of Physical Sciences and Engineering, Australian National University, ACT 0200 Canberra, Australia*
[2]*Photonics and Mathematical Optics Group, Tecnológico de Monterrey, Monterrey, Mexico*

dnn124@rsphysse.anu.edu.au

Abstract: We generate higher-order azimuthally modulated Bessel optical lattices in photorefractive crystals by employing a phase-imprinting technique. We report on the experimental observation of self-trapping and nonlinear localization of light in such segmented lattices in the form of ring-shaped and single-site states. The experimental results agree well with numerical simulations accounting for an anisotropic and spatially nonlocal nonlinear response of photorefractive crystals.

OCIS codes: (190.4420) Nonlinear optics, transverse effects in; (190.5940) Self-action effects.

References and links

1. Yu. S. Kivshar and G. P. Agrawal, *Optical Solitons: From Fibers to Photonic Crystals* (Academic Press, San Diego, 2003).
2. D. N. Christodoulides, F. Lederer, and Y. Silberberg, "Discretizing light behaviour in linear and nonlinear waveguide lattices," Nature **424,** 817–823 (2003).
3. N. K. Efremidis, S. Sears, D. N. Christodoulides, J. W. Fleischer, and M. Segev, "Discrete solitons in photorefractive optically induced photonic lattices," Phys. Rev. E **66,** 046602–5 (2002).
4. J. W. Fleischer, M. Segev, N. K. Efremidis, and D. N. Christodoulides, "Observation of two-dimensional discrete solitons in optically induced nonlinear photonic lattices," Nature **422,** 147–150 (2003).
5. D. Neshev, E. Ostrovskaya, Y. Kivshar, and W. Krolikowski, "Spatial solitons in optically induced gratings," Opt. Lett. **28,** 710–712 (2003).
6. H. Martin, E. D. Eugenieva, Z. G. Chen, and D. N. Christodoulides, "Discrete solitons and soliton-induced dislocations in partially coherent photonic lattices," Phys. Rev. Lett. **92,** 123902–4 (2004).
7. Y. V. Kartashov, V. A. Vysloukh, and L. Torner, "Rotary solitons in Bessel optical lattices," Phys. Rev. Lett. **93,** 093904–4 (2004).
8. X. Wang, Z. Chen, and P. G. Kevrekidis, "Observation of discrete solitons and soliton rotation in optically induced periodic ring lattices", Phys. Rev. Lett. **96,** 083904–4 (2005).
9. J. Durnin, "Exact solutions for nondiffracting beams. I. The scalar theory," J. Opt. Soc. Am. A **4,** 651–654 (1987).
10. J. Durnin, J. J. Miceli, Jr., and J. H. Eberly, "Diffraction-free beams," Phys. Rev. Lett. **58,** 1499–1501 (1987).
11. Y. Lin, W. Seka, J. H. Eberly, H. Huang, and D. L. Brown, "Experimental investigation of bessel beam characteristics," Appl. Opt. **31,** 2708–2713 (1992).
12. T. Wulle and S. Herminghaus, "Nonlinear optics of bessel beams," Phys. Rev. Lett. **70,** 1401–1404 (1993); Erratum: Phys. Rev. Lett. **71,** 209 (1993).
13. C. Lopez-Mariscal, J. C. Gutierrez-Vega, and S. Chavez-Cerda, "Production of high-order Bessel beams with a Mach-Zehnder interferometer," Appl. Optics **43,** 5060–5063 (2004).
14. N. Chattrapiban, E. A. Rogers, D. Cofield, W. T. Hill, III, and R. Roy, "Generation of nondiffracting Bessel beams by use of a spatial light modulator," Opt. Lett. **28,** 2183–2185 (2003).
15. S. H. Tao, W. M. Lee, and X. C. Yuan, "Dynamic optical manipulation with a higher-order fractional Bessel beam generated from a spatial light modulator," Opt. Lett. **28,** 1867–1869 (2003).

#10394 - $15.00 USD Received 23 January 2006; revised 17 March 2006; accepted 18 March 2006

16. D. McGloin and K. Dholakia, “Bessel beams: diffraction in a new light,” Contemp. Phys. **46,** 15–28 (2005).
17. D. McGloin, G. C. Spalding, H. Melville, W. Sibbett, and K. Dholakia, “Applications of spatial light modulators in atom optics,” Opt. Express **11,** 158–166 (2003), http://www.opticsexpress.org/abstract.cfm?URI=OPEX-11-2-158.
18. Y. V. Kartashov, A. A. Egorov, V. A. Vysloukh, and L. Torner, “Stable soliton complexes and azimuthal switching in modulated Bessel optical lattices,” Phys. Rev. E **70,** 065602–4 (2004).
19. A. A. Zozulya, D. Z. Anderson, A. V. Mamaev, and M. Saffman, “Solitary attractors and low-order filamentation in anisotropic self-focusing media,” Phys. Rev. A **57,** 522–534 (1998).
20. A. S. Desyatnikov, D. N. Neshev, Yu. S. Kivshar, N. Sagemerten, D. Trager, J. Jagers, C. Denz, and Y. V. Kartashov, “Nonlinear photonic lattices in anisotropic nonlocal self-focusing media,” Opt. Lett. **30,** 869–871 (2005).
21. G. Indebetouw, “Nondiffracting optical fields: some remarks on their analysis and synthesis,” J. Opt. Soc. Am. A **6,** 150–152 (1989).
22. A. Vasara, J. Turunen, and A. T. Friberg, “Realization of general nondiffracting beams with computer-generated holograms,” J. Opt. Soc. Am. A **6,** 1748–1754 (1989).
23. W. X. Cong, N. X. Chen, and B. Y. Gu, “Generation of nondiffracting beams by diffractive phase elements,” J. Opt. Soc. Am. A **15,** 2362–2364 (1998).
24. J. Rogel-Salazar, G. H. C. New, and S. Chavez-Cerda, “Bessel-Gauss beam optical resonator,” Opt. Commun. **190,** 117–122 (2001).
25. R. Fischer, D. Träger, D. N. Neshev, A. A. Sukhorukov, W. Krolikowski, C. Denz, and Yu. S. Kivshar, “Reduced-symmetry two-dimensional solitons in square photonic lattices,” Phys. Rev. Lett. **96**, 023905(4) (2006).

1. Introduction

In recent decades, many studies have been devoted to the analysis and experimental observation of self-trapping and localization of light in different types of nonlinear media [1]. The self-trapped states, often referred to as spatial optical solitons, are highly robust and may exhibit particle-like behavior in interactions, what makes them promising objects for the beam control and all-optical switching. The presence of periodically varying refractive index in the medium affects the propagation and localization of optical beams, and many recently observed new effects are associated with the soliton dynamics in periodic waveguide arrays [2]. As was recently suggested theoretically [3] and demonstrated in experiments [4, 5, 6], a periodically modulated refractive index can be induced by imprinting an optical pattern in a photorefractive crystal, and nonlinear localized states can exist in different spectral bands of the periodic lattices. Many novel effects have also been predicted to occur in nondiffracting ring Bessel-like optical lattices [7], and the first experimental results on the ring lattices have been obtained very recently [8].

Nondiffracting optical beams appear as a special class of linear modes propagating in the free space without any distortion [9]. The simplest example of the nondiffracting beams has the amplitude profile proportional to the zero-order Bessel function, and therefore such beams are often called *Bessel beams*. In spite of the fact that the Bessel beams appear as eigenmode solutions of Maxwell’s equations of infinite transverse extent and energy, they have been demonstrated in experiments with finite beams, where the characteristics of stationary propagation are sustained over long distances [10, 11, 12, 13].

The purpose of this paper is twofold. First, we report on our experimental results on the generation of different types of nondiffracting Bessel optical beams by employing a phase-imprinting technique [14, 15] and concentrate on azimuthally modulated Bessel beams. Second, we use the nondiffracting nature of the Bessel beam to induce an optical lattice in a biased photorefractive crystal and study the nonlinear trapping of light in such lattices. While nondiffracting beams are extensively used for optical manipulation of particles [16] and atoms [17], we demonstrate that due to the nonlinear self-focusing response of the material “optical trapping of light” is also possible. We report on the first experimental observation of self-focusing and localization of light in azimuthally modulated Bessel lattices considered theoretically [18]. In particular, we generate experimentally different types of localized states positioned symmetrically or asymmetrically with respect to the segmented Bessel lattice. We show that our ex-

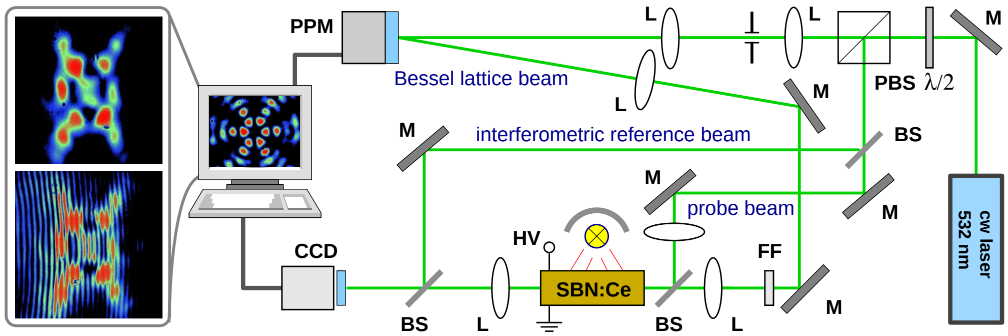

Fig. 1. Schematic structure of the experimental setup for generating the modulated Bessel-like beams with a phase imprinting: PPM – programmable phase modulator; PBS – polarizing beam splitter; $\lambda/2$ – half-wave plate; L – lenses; M – mirrors; BS – beam splitter; FF – Fourier filter; SBN –photorefractive crystal, Strontium Barium Niobate; CCD – camera. Inset on the left: Images of the Bessel lattice, localized state, and its interferogram.

perimental results are in a good agreement with numerical simulations of the nonlinear model accounting for a nonlocal anisotropic response of photorefractive nonlinear crystals [19, 20].

2. Generation of nondiffracting Bessel lattices

A Bessel beam is associated with a solution of the wave equation such that any cross-section of the beam intensity distribution remains independent of the propagation variable z, and it can be presented as a superposition of an infinite number of plane waves. In past years, a number of practical ways to generate Bessel beams have been suggested including the use of passive optical systems such as ring apertures, Fabry-Perot etalons, and axicons [21], as well as holographic methods [22], or diffractive phase elements [23]. In contrast to passive methods, several active schemes have been proposed to produce finite-aperture approximations of different Bessel and Bessel-Gauss beams in resonators [24]. Here, we generate nondiffracting Bessel-like optical beams based on the phase-imprinting technique [14, 15]. We then study the propagation and self-action of probe beams in optical lattices induced by such Bessel beams.

In our experiments we employ a programmable phase modulator (PPM), as shown in the setup scheme [Fig. 1]. In this arrangement, the beam from a frequency-doubled cw Nd:YVO_4 laser (532 nm) is split into two orthogonally polarized beams by a polarizing beam splitter (PBS), where the splitting ratio is set by a half-wave plate. The beam transmitted through the PBS is expanded approximately 10 times and illuminates a phase modulator (Hamamatsu X8267). The modulator is programmed to reproduce the exact phase profile of a modulated Bessel beam given by

$$E(r,\varphi) = E_0 J_n(\rho/w)\cos(n\varphi), \tag{1}$$

where ρ and φ are the transverse polar coordinates, w is the spatial scale, and J_n is the n-th order Bessel function. Such a field distribution represents a well-known nondiffracting beams, and it is ideal for the application of the optical induction technique in a similar way as realized earlier for square lattices induced by four interfering beams [4, 25].

In practice, the input pattern distribution is superimposed onto a broad Gaussian carrier beam and the constant (nondiffracting) intensity profile can be preserved only for a finite distance (i.e., the focal region), which in our case for $w = 7.6\,\mu$m is of the order of 2 cm. In fact, the phase modulator only reproduces the phase structure of the Bessel beam (1) and to obtain a real nondiffracting beam we employ Fourier filtering in the focal plane of the telescope which im-

#10394 - $15.00 USD Received 23 January 2006; revised 17 March 2006; accepted 18 March 2006

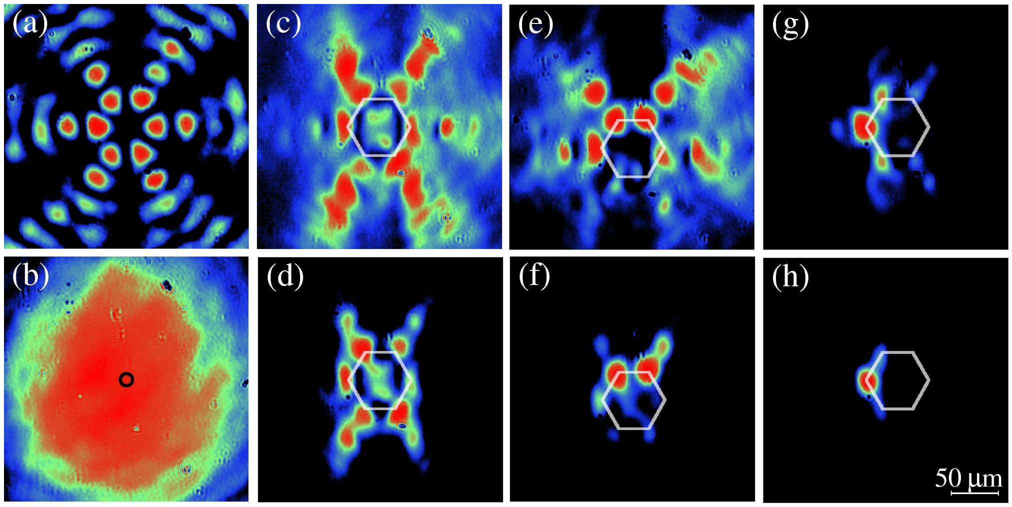

Fig. 2. Experimental images: (a) Intensity profile of the generated third-order Bessel lattice; (b) linear diffraction of the probe beam without the ilattice, the outer radius of the black circle shows the size of the input beam at the crystal front facet; (c-h) linear diffraction (top row) and nonlinear self-focusing (bottom row) of the input beam positioned (c,d) at the lattice center, (e,f) between two cites, and (g,h) at one site of the first lattice ring.

ages the active plane of the modulator onto the front face of a 20 mm long SBN photorefractive crystal. The crystal is externally biased by a DC electric field (3500 V/cm) applied horizontally along the crystal c-axis, allowing the study of self-action effects.

3. Light localization in a Bessel lattice

The Bessel beam forming the lattice [Fig. 2(a)] is ordinary polarized and its stationary propagation inside the crystal is not affected by the applied voltage, due to a small value of the electro-optic coefficient for this polarization. On the other hand, an extraordinary polarized probe beam feels the Bessel-type potential, and it experiences strong self-action due to the self-focusing nonlinearity of a photorefractive crystal [3, 4, 5, 6]. As a probe, we use the beam reflected from the PBS, which is combined with the lattice onto a beam splitter and is tightly focused to a size of 13.2 μm onto the front face of the crystal. The input and output crystal faces can be imaged by a lens and recorded onto a CCD camera for analyzing the transverse intensity distribution. Additionally, a small portion of the probe beam is used as an interferometric reference beam to monitor the phase profile of the probe beam at the output.

Without the lattice, the narrow input probe beam [indicated by a circle in Fig. 2(b)] diffracts and greatly increases its size to 162 μm at the crystal output, as shown in Fig. 2(b), which corresponds to 12 diffractions lengths of propagation. Then we switch on the PPM, which is programmed to reproduce the phase distribution of the Bessel beam [Eq. (1)]. The resulting intensity distribution of this lattice forming beam (after Fourier filtering) has the form shown in Fig. 2(a). Under the action of the bias electric field this beam induces a refractive index change following its intensity profile. It is important to note that we have to select the proper orientation of the lattice pattern with respect to the crystalline c-axis, in order to minimize the distortion of the refractive index modulation due to the anisotropy of the photorefractive crystal as previously discussed for square lattices [20]. In our case of horizontal bias field, we find that the optimal orientation corresponds to a zero intensity line of the Bessel pattern perpendicular to

#10394 - $15.00 USD Received 23 January 2006; revised 17 March 2006; accepted 18 March 2006

the electric field, as shown in Fig. 2(a). Still the anisotropy of the nonlinear response cannot be completely eliminated, and it affects the propagation of the probe beam. This effect is different for the Bessel lattice of different orders. In our experiments, we have tested the azimuthally modulated Bessel lattices of the orders $n = 1,2,3$, and 4. For the low-order lattices, the two ($n = 1$) or four ($n = 2$) sites in the inner ring dominate the structure of induced refractive index and represent almost decoupled waveguides for the probe beam. For the higher-order Bessel beams ($n = 4$) the effect of the crystal anisotropy leads to strong vertical merging of the closely located lattice sites. Therefore, below we present results for the representative example of the third-order modulated Bessel beams ($n = 3$).

When the probe beam propagates in the direction of the generated Bessel lattice, at low laser powers (20 nW) the beam experiences discrete diffraction with the output profiles strongly dependent on the specific location of the initial excitation. This can be seen in Fig. 2(c) for the excitation in the origin of the lattice, between two lattice sites in (e), and on a single lattice site in (g). At high beam power (250 nW) the beam experiences nonlinear self-focusing and becomes localized at the six sites of the first ring of the Bessel lattice [Figs. 2(d)-(h)].

We note that the nonlinear response of a biased photorefractive crystal is anisotropic and the effect of anisotropy is clearly visible. It results in a deformation of the induced Bessel-type potential and, correspondingly, in an asymmetry of the output beam profile for the case of symmetric excitation, when the input beam is positioned at the lattice center [Figs. 2(c,d)]. We see that in the low-power regime [Fig. 2(c)] the beam spreads faster in the vertical direction, indicating that the lattice potential is stronger along the horizontal axis, coinciding with the direction of the external bias field.

Further, we tested the nonlinearity-induced localization of the probe beam when the input is offset from the lattice center. For the input position between two upper sites of the main ring we observed beam localization at the power level of 600 nW in the form of a double-peak in-phase structure [Fig. 2(f)]. For the same excitation at low powers (20 nW) the beam diffracts as shown in Fig. 2(e). Based on the generic properties of lattice solitons [1, 2] and results of numerical simulations, we expect that the double-peak states may be unstable with respect to symmetry breaking. When the input probe beam is positioned onto a lattice site of the first ring, the beam diffracts for a low power [20 nW - Fig. 2(g)] and localizes to a single lattice site at a larger power [450 nW - Fig. 2(h)]. In all the cases (d), (f), and (h), the light localized on first lattice ring was in-phase as interferometrically tested, while the residual light in the lattice centre appears weakly phase shifted as shown in the inset of Fig. 1. This phase shift is attributed to fact that this residual light is propagating in a low refractive index region of the lattice.

4. Numerical results for the anisotropic model

In order to confirm the existence of localized states corresponding to the experimental observations, we solve numerically the extended model accounting for anisotropic and nonlocal nonlinear response of the photorefractive material [19]. This model describes the propagation of the electric field envelope,

$$i\partial_z E + \nabla^2 E + \gamma \partial_x \varphi E = 0, \tag{2}$$

coupled to the electrostatic potential φ of the optically-induced space-charge field that satisfies the relation [19]:

$$\nabla^2 \varphi + \nabla \varphi \nabla \ln(1+I) = \partial_x \ln(1+I). \tag{3}$$

Here $\nabla^2 = \partial_x^2 + \partial_y^2$ and physical variables $\tilde{x}$, $\tilde{y}$, and $\tilde{z}$ correspond to their dimensionless counterparts as $(\tilde{x},\tilde{y}) = (wx, wy)$ and $\tilde{z} = 2\kappa w^2 z$, here w is the transverse scale factor [Eq. (1)] and $\kappa = 2\pi n_0/\lambda$ is the carrier wave vector with the linear refractive index n_0. Parameter $\gamma = w^2\kappa^2 n_0^2 r_{\text{eff}}\mathscr{E}$ is defined through the effective electro-optic coefficient r_{eff} and externally

#10394 - $15.00 USD
Received 23 January 2006; revised 17 March 2006; accepted 18 March 2006

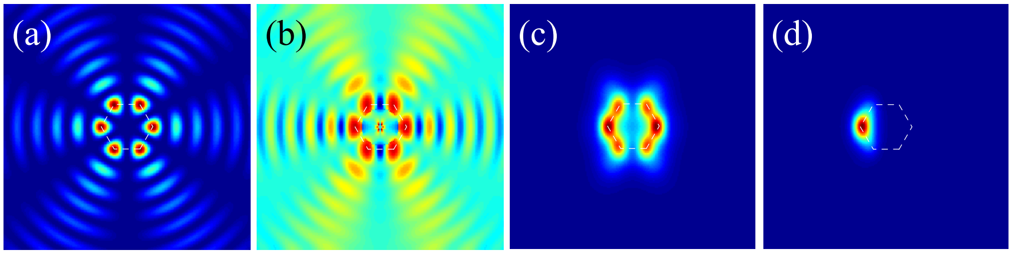

Fig. 3. Results of numerical simulations with the anisotropic nonlocal model Eqs. (3)-(5): (a) Intensity of the azimuthally modulated Bessel beam and (b) corresponding induced refractive index profile $\sim \partial_x \varphi$; parameters are $A = 2.5$ and $\gamma = 2$. (c,d) Examples of the ring-like and single-site solitons corresponding to the experimental data shown in Figs. 2(d) and (h), respectively. The soliton with $\beta = 0.13$ and the peak intensity $\max|E|^2 = 0.05$ in (c) is close to the bifurcation point from the corresponding linear guided wave, while the soliton in (d) with $\beta = 0.3$ and $\max|E|^2 = 0.97$ is essentially in the nonlinear regime.

applied bias DC field $\mathscr{E}$. The total intensity is given by the sum

$$I = |E|^2 + A^2 J_3^2(r) \cos^2(3\varphi) \tag{4}$$

where $r^2 = x^2 + y^2$, $\varphi = \tan^{-1} y/x$, and I is measured in units of the background illumination intensity, necessary for the formation of spatial solitons in such a medium. We solve Eqs. (3), (4) and find that the modulated Bessel beam induces the refractive index modulation which has a symmetry lower than the symmetry of the intensity pattern [cf. Fig. 3(a) and (b)]. Stationary solutions of the system (2), (3) are sought in the standard form $E(x,y,z) = U(x,y)\exp(i\beta z)$, where the real envelope U satisfies the equation

$$-\beta U + \nabla_\perp^2 U + \gamma \partial_x \varphi U = 0. \tag{5}$$

To find localized solutions to the system Eqs. (3), (5) we apply the relaxation technique [19] with initial profile in the form of a Gaussian ansatz. When the Gaussian profile is positioned in the origin of the induced potential, we find numerical solutions for ring-shaped solitons [Fig. 3(c)], which closely resemble the localized states observed in the experiment [Fig. 2(d)]. However, if the propagation constant β exceeds some threshold, which corresponds to the threshold for soliton power and peak intensity, our relaxation procedure converges to the on-site single soliton, shown in Fig. 3(d). We conclude that two families of solutions may be linked through a bifurcation, which may correspond to the onset of symmetry-breaking instability for the effectively two-lobe "in-phase" soliton shown in Fig. 3(c).

5. Conclusions

We have generated modulated Bessel-type optical lattices in a photorefractive crystal by employing a phase-imprinting technique. We have studied the nonlinear light propagation and self-action in such segmented Bessel lattices and observed light localization in the form of ring-shaped and single-site self-trapped localized states. The results are in a good agreement with numerical simulations of the nonlinear model accounting for a nonlocal anisotropic response of photorefractive nonlinear crystals.

Acknowledgments

This work has been supported by the Australian Research Council. The authors thank Zhigang Chen for discussions and a copy of the paper [8] made available to us prior its publication.